Journal of Mines, Metals and Fuels, *73(6): 1651-1662; 2025. DOI: 10.18311/jmmf/2025/48770*

Print ISSN : 0022-2755

Journal of Mines, Metals and Fuels

Contents available at: *www.informaticsjournals.co.in/index.php/jmmf*

Numerical Investigation of Chassis Torsional Stiffness for Formula Student Vehicles

Bhumin A. Gala, Deev Munani, Kartik P. Mandaliya, Tanvi Talekar, Hari Vasudevan and Vinayak H. Khatawate*

Department of Mechanical Engineering, SVKM's Dwarkadas J. Sanghvi College of Engineering, Vile Parle, Mumbai - 400056, Maharashtra, India; vinayak.Khatawate@djsce.ac.in

Abstract

This study examines the torsional rigidity of a Formula Student race car's space frame chassis using computer-aided tools, guided by modifications based on the latest FSAE rulebook. Torsional rigidity is essential in chassis design, impacting vehicle handling, safety, and durability. By increasing rigidity, chassis flex under load is minimized, resulting in improved control and a more robust structure, critical for high-performance applications. Finite Element Analysis (FEA) software was used to simulate torsional rigidity tests, applying a standard 25 N load at each suspension point. Parameters, such as material properties, geometry, and load positioning were controlled to mimic real-world conditions. Different chassis configurations were analyzed to assess the effect of design changes on torsional rigidity. Results showed that incorporating cross tubes at specific chassis points significantly enhanced rigidity, with optimal load transfer achieved by adjusting tube dimensions and angles. Designs with reinforced cross members and strategically selected materials achieved the highest rigidity values. The calculations obtained from FEA were also verified through physical testing, ensuring the accuracy and reliability of the simulation results. The findings demonstrate how simulation-based analysis can guide design modifications to improve vehicle performance and structural durability.

Major Findings: *The study used Finite Element Analysis (FEA) to evaluate and optimize the torsional rigidity of a Formula Student chassis, ensuring compliance with FSAE regulations. The simulation findings were validated through physical testing, confirming the reliability of FEA in guiding chassis design improvements for better handling and performance.*

Keywords: *Chassis, Computational Mechanics, Finite Element Analysis (FEA), Stability, Torsion, Torsional Rigidity*

1.0 Introduction

The structural design of a Formula Student race car's chassis plays a critical role in its overall performance, handling, and safety[1,2]. The chassis is one of the most crucial load-bearing components, and it must be rigid enough to endure shocks, twisting, vibrations, and other stresses. In addition to strength, ensuring sufficient bending and torsional stiffness is essential for better handling performance[2]. Therefore, both strength and stiffness are key factors in designing a chassis. Among the key design parameters, torsional rigidity is essential, as it minimizes chassis flex under load, ensuring better control and stability during high-speed maneuvers. Torsional rigidity refers to a structure's resistance to twisting when subjected to torque[3]. It is a critical parameter in chassis design, as higher torsional rigidity reduces deformation under load, leading to improved handling, stability, and durability[4]. Hence, a thorough analysis is necessary to assess the overall strength, ensuring optimal performance during operation[5].

*Author for correspondence

2.0 Theoretical Calculations

To estimate the required chassis stiffness, the chassis was modeled in series with the front and rear suspension systems, as shown in the Figure below. Figure 1 illustrates the equivalent stiffness model of the suspension and chassis, representing the anti-roll stiffness.

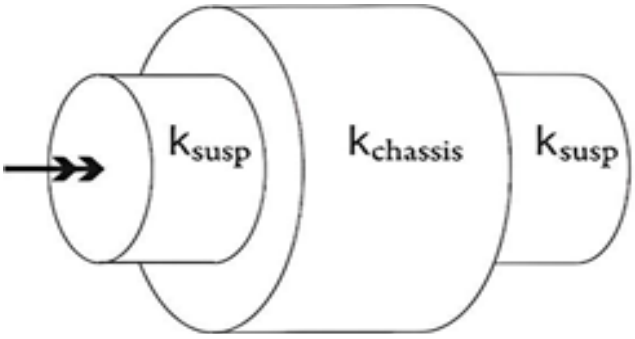


Figure 1. Equivalent stiffness model of suspension and chassis.

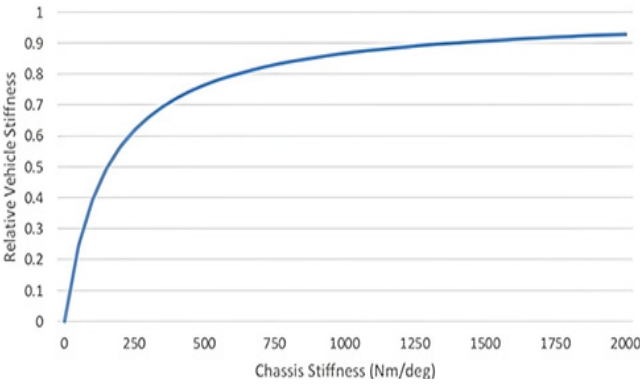


Figure 2. Graph of chassis stiffness vs relative vehicle stiffness[6].

The resistance to torsion at the suspension is represented by the anti-roll stiffness, allowing the total vehicle stiffness to be plotted as a function of chassis stiffness. Figure 2 depicts the relationship between chassis stiffness and relative vehicle stiffness. It is demonstrating the impact of increasing chassis stiffness on overall vehicle rigidity. Since the chassis and suspension act in series, the total vehicle stiffness (k_{veh}) is governed by the following formulation:

$$k_{veh} = \left(\frac{1}{k_f} + \frac{1}{k_{ch}} + \frac{1}{k_r}\right)^{-1} \quad (1)$$

The variation of chassis stiffness as a function of relative vehicle stiffness follows a nonlinear trend, as depicted in Figure 2[6]. Reduced handling performance and increased deformation under torsional loads result from excessive chassis flex, which limits the overall vehicle stiffness at lower chassis stiffness values. Relative vehicle stiffness rises in tandem with chassis stiffness, improving handling characteristics and lowering structural deflection. Beyond 90% of the rigid case, however, additional chassis stiffness increases lead to diminishing returns, where the suspension system becomes the limiting factor in the overall structural response. This behavior suggests that although performance is improved by a stiffer chassis but significantly increasing weight, making such improvements less feasible.

Considering these conditions, the minimum torsional stiffness of the chassis was calculated to balance performance and weight effectively. The relative stiffness, k_{rel}, is defined as the ratio of chassis stiffness k_{ch} to suspension stiffness k_{susp} :

$$k_{rel} = \frac{k_{ch}}{k_{susp}} \quad (2)$$

Since the chassis and suspension act in series, the total vehicle stiffness k_{veh} is determined as:

$$\frac{1}{k_{veh}} = \frac{1}{k_f} + \frac{1}{k_r} + \frac{1}{k_{ch}} \quad (3)$$

where k_f and k_r are the stiffness of the front and rear suspensions, respectively, and *kch* is the chassis stiffness.

To achieve a relative stiffness of 90% of the rigid case ($k_{rel} = 0.9$), the relationship becomes[7]

$$k_{ch} = 9 * k_{susp} \quad (4)$$

This calculation indicates that the chassis stiffness must be nine times the suspension stiffness to ensure optimal vehicle performance without unnecessary weight penalties.

k_f = 441.23 Nm/deg

k_r = 387.83 Nm/deg

$\therefore k_{susp} = 207.115 \frac{\text{Nm}}{\text{deg}}$

From Equation (4)

$$k_{ch} = 1864.035 \text{ N m/d eg}$$

Based on the above calculations, it can be concluded that a minimum torsional stiffness of 1864.035 Nm/deg is required for the chassis design to ensure adequate structural integrity and performance under operational conditions.

3.0 Methodology

The chassis was modeled and analyzed using ANSYS to simulate its structural behavior under real-world conditions. While composite materials are increasingly used in modern automotive applications due to their high strength-to-weight ratio, AISI 1018 steel was chosen for the chassis design due to its cost-effectiveness, manufacturability, and mechanical properties that align with Formula Student vehicle requirements. The selection of chassis material is crucial in balancing stiffness, durability, manufacturability, and cost[8], all of which play a significant role in student motorsport competitions. Because of its high yield strength and good elongation, AISI 1018 steel guarantees that the chassis can sustain high bending and torsional stresses while still having some ductility to absorb impact loads. For Formula Student teams that regularly revise and alter their designs, AISI 1018 steel is perfect because it is simple to weld, machine, and repair, unlike composites, which call for specific fabrication methods and bonding processes. Although Carbon Fiber-Reinforced Polymers (CFRP) reduce weight, they have drawbacks, including expensive production costs, drawn-out fabrication processes, and challenges with structural repairs. They also require sophisticated finite element modeling techniques to accurately predict failures. Furthermore, regulatory compliance and safety considerations favor the use of steel in Formula Student competitions[9]. The FSAE rulebook mandates minimum material strength requirements for chassis structures, which AISI 1018 steel meets while maintaining an optimal balance between rigidity and weight. Given the constraints of Formula Student, where rapid prototyping, cost efficiency, and reliability are critical, AISI 1018 steel remains a practical and robust choice over composites for chassis applications. Key points were defined to outline the geometry, which were then connected to form the framework of the chassis. A 3D line mesh was generated, with mesh density tailored to different beam types for precise stress and deformation analysis. Figure 3 shows the 3D modeling and meshing of the chassis structure as used in the analysis.

To accurately simulate the structural response of the chassis under torsional loading, appropriate boundary conditions were applied in the Finite Element Analysis (FEA) setup. As depicted in Figure 4, the chassis was constrained at specific locations to replicate real-world mounting conditions and ensure accurate stiffness evaluation. The boundary conditions used in the simulation can be categorized as follows:

1. Fixed Boundary Conditions (Fully Constrained Nodes)
    - One end of the chassis was fully constrained (fixed in all degrees of freedom) to simulate the attachment points to the vehicle structure. This prevents any translational or rotational movement, ensuring that the applied load induces a torsional effect rather than rigid body motion.
    - The constrained nodes correspond to the suspension mounting points at one end, mimicking real-world constraints experienced by a vehicle chassis.
2. Torque Application and Force Constraints
    - A 100 N force was applied at specific suspension mounting locations to replicate reaction forces generated during cornering. The applied forces created a twisting moment about the chassis' central axis, enabling torsional stiffness evaluation.
    - The torque was applied through the upright points, while the opposite end of the chassis remained constrained to isolate the torsional response.
3. Elimination of Suspension Compliance
    - The dampers were modeled as rigid links to remove suspension flex and ensure that the stiffness measurement represented only the chassis contribution. This prevents additional deflections that could interfere with the analysis of structural rigidity.

- The suspension attachment points were constrained to restrict unwanted lateral or vertical movement, thereby focusing the analysis on pure torsional deformation.

The implementation of these boundary conditions ensures that the simulation accurately replicates the real-world torsional stiffness test setup, where one end of the chassis is rigidly fixed, while a torque is applied at the other end.

Based on actual vehicle dynamics, specifically the reaction forces encountered during cornering, a 100N force is applied in the Finite Element Analysis (FEA) of the chassis torsional stiffness. The loads transmitted through the suspension mounting points under normal cornering circumstances in a Formula Student vehicle are used to calculate this force value. The approach adheres to accepted FEA simulation procedures, in which the structural response is assessed by applying a controlled load at strategic locations.

The 100N force in this instance mimics the reaction forces brought on by lateral acceleration during cornering maneuvers. A torsional moment about the chassis is produced by the applied force, enabling a numerical evaluation of stiffness. The simulation successfully isolates the chassis' structural contribution while removing the effects of suspension compliance by restricting one end of the chassis and applying force at the suspension mounting points.

By examining the normal forces operating on a Formula Student suspension system, which are derived from empirical force distribution calculations, the selection of 100N is confirmed. To ensure that the

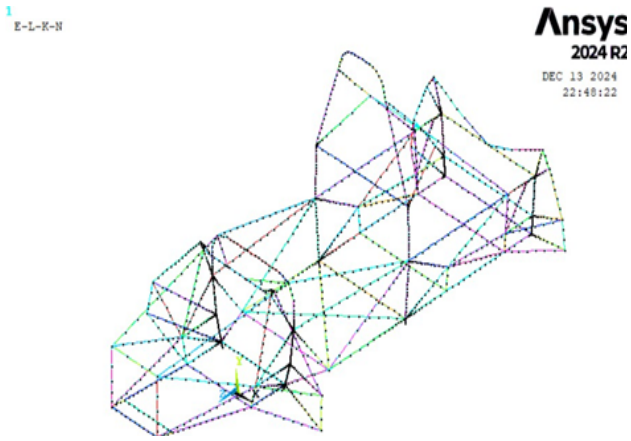


Figure 3. Modelling and meshing of chassis.

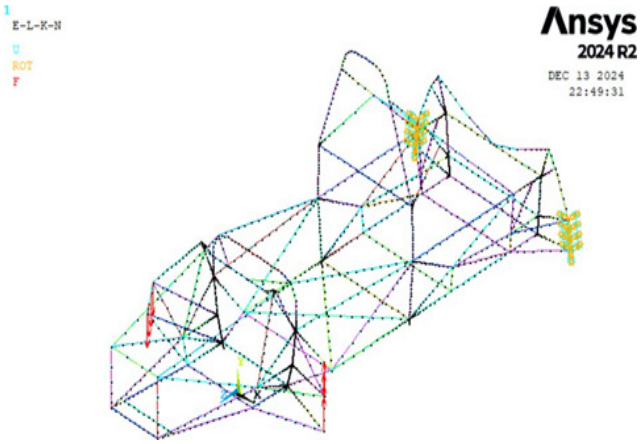


Figure 4. Boundary conditions.

applied force accurately reflects real-world loads, these calculations take into account the lateral forces on tires during dynamic conditions like braking and cornering. This force magnitude is further supported by experimental validation, which verifies that the applied load is representative of the forces the chassis actually experiences during operation by taking physical deflection measurements.

Parameters, such as material properties, geometry, and load positioning were carefully controlled within ANSYS to replicate operational conditions. Figure 4 details the boundary conditions applied during the ANSYS simulation, ensuring accurate replication of real-world conditions.

The analysis included multiple chassis configurations to evaluate the impact of design modifications on torsional rigidity. Results indicated that incorporating cross tubes at strategic points significantly enhanced rigidity, with optimal load transfer achieved through adjustments in tube dimensions and angles. Designs featuring reinforced cross members and the use of AISI 1018 steel achieved the highest rigidity values[10]. ANSYS simulations provided valuable insights into the torsional behavior of the chassis, enabling effective refinements to optimize performance, durability, and weight efficiency[11].

3.1 Mesh Convergence Study

To ensure the accuracy and reliability of the Finite Element Analysis (FEA) results, a mesh convergence study was performed. The analysis began with a coarse mesh, consisting of approximately 800 elements, and

the mesh density was progressively refined to observe its effect on the calculated torsional stiffness. However, the selection of the appropriate element type plays a crucial role in ensuring computational efficiency and accuracy.

The chassis is modeled using Beam188, a two-node beam element, in ANSYS APDL. This element has been chosen as this is most compatible with space frame structures, in which the main load paths are through connected tubular member. The beam elements capture the axial, bending and torsional behavior at a much lower computational cost compared to solid or shell elements. Also, it provides six DOFs each for all the nodes, enabling a precise simulation of how the structure responds to the applied loads. The use of Beam188 elements ensured that the finite element model adequately replicated real-world chassis stiffness characteristics while achieving an optimal balance between computational efficiency and result accuracy.

The results showed significant variation with the initial coarse mesh, but as the number of elements increased, the variation reduced and the results began to stabilize. At 1657 elements, the torsional stiffness value converged to approximately 2600 Nm/deg, with less than 0.1% change observed upon further refinement to 2000 and 2500 elements. This confirmed that the solution had become independent of mesh density, and any additional refinement would result in negligible accuracy improvements, while increasing computational time. Therefore, the mesh with 1657 elements was chosen for all further simulations, as it provided an optimal balance between result accuracy and computational efficiency.

Table 1. Mesh convergence study results

Number of Elements	Torsional Stiffness (Nm/deg)	Change (%)
800	2300	0
1200	2500	8.7
1657	2600	4.0
2000	2601	0.03
2500	2602	0.01

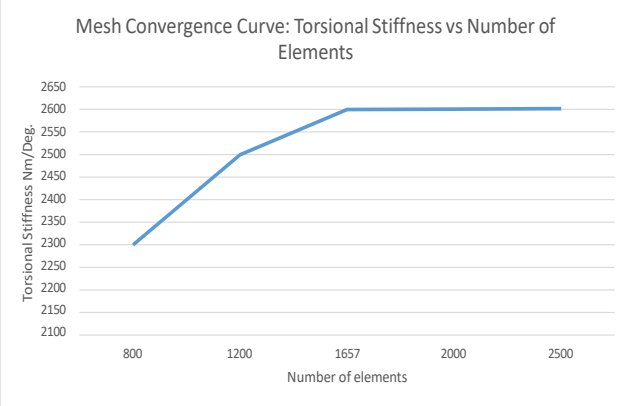


Figure 5. Graph of torsional stiffness vs number of elements used in simulation.

The results of the mesh convergence study are summarized in Table 1.

From Table 1, it can be observed that beyond 1657 elements, the variation in torsional stiffness becomes negligible (less than 0.1%). This demonstrates that the solution has converged, and further refinement would result in an unnecessary increase in computational time without any significant improvement in accuracy. As Figure 5 states, the torsional stiffness stabilizes at 1657 elements, indicating mesh convergence where further refinement yields negligible changes in the results.

4.0 Analysis

One of the most precise methods for determining the torsional stiffness of the chassis involves measuring it at the hub faces. A model of the chassis, including suspension arms and geometry, is created with the aid of beams. The A-arms are used to apply the required load, and the compliance of the suspension system is incorporated into the analysis. Since all stresses acting on the vehicle are transmitted through the suspension, it is crucial to evaluate the stiffness of the chassis and suspension components as an integrated structure.

In this approach, the dampers were modeled as rigid links, and the weights were applied at the rear upright pivot points, which were constrained in all directions. Since the primary objective of the study was to evaluate the structural response of the chassis alone,

the influence of damping elements had to be excluded. Dampers give the suspension system flexibility, which may cause more deflections and have an impact on the chassis stiffness measurement. By substituting rigid links for them, the analysis separates the chassis' contribution to the total stiffness and gives a more accurate picture of its torsional rigidity. The fact that torsional stiffness is largely determined by the chassis and suspension geometry rather than damper compliance in real-world vehicle dynamics further supports the choice to model dampers as rigid links. The damper movement absorbs transient loads and vibrations under dynamic conditions, but it does not substantially contribute to the rigid body torsion of the chassis during static torsional stiffness testing.

The deflection at each pivot point was then measured. Similarly, for the front, the rear upright pivot points were restricted in all degrees of freedom, and a torque was applied at the front through the upright points to assess the torsional stiffness at the front of the chassis. This method provides a comprehensive evaluation of the chassis and suspension stiffness as a unified system[12]

To calculate the torsional stiffness of the chassis, one side (either the front or rear) was fixed, while the stiffness of the opposite side was evaluated[13]. By constraining one side of the chassis, the resulting deflections and torsional behavior of the free side were measured, allowing for an accurate assessment of the chassis stiffness in response to applied loads. This approach helped isolate the torsional stiffness characteristics of each section, providing valuable insights into the overall rigidity of the chassis structure. Figures 6 and 7 illustrate the setups used for calculating the torsional stiffness of the chassis, with Figure 6 showing the front suspension fixed to assess the rear suspension stiffness and Figure 7 depicting the rear suspension fixed to evaluate the front suspension stiffness.

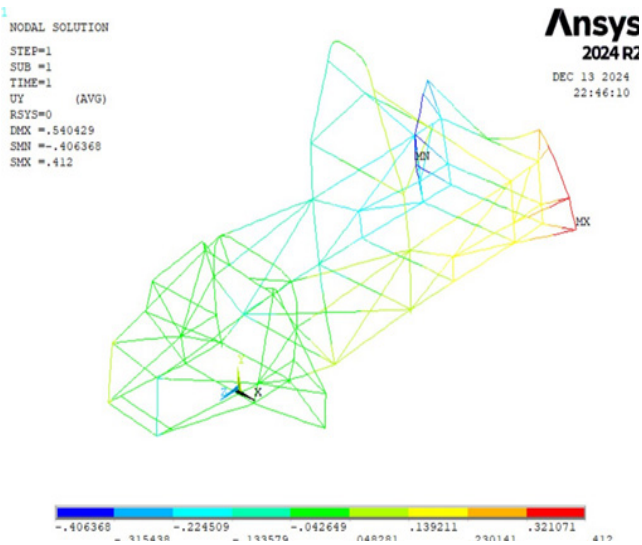


Figure 6. Front suspension is fixed to calculate rear suspension stiffness.

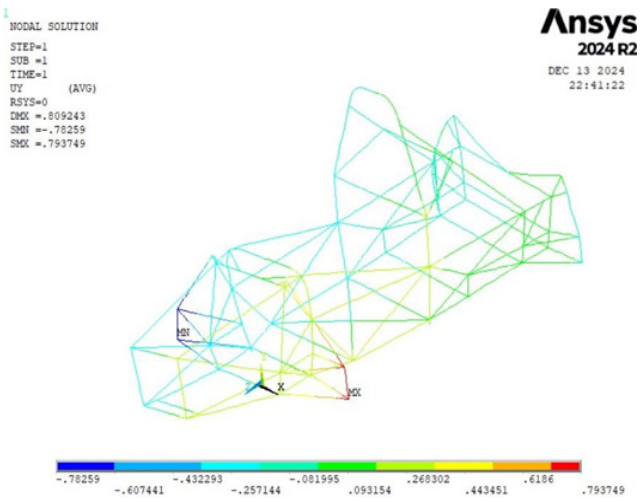


Figure 7. Rear suspension is fixed to calculate front suspension stiffness.

4.1 Mathematical Analysis

The torsional stiffness k is given by

$$k = \frac{T}{\theta}$$

T = Torque applied = Applied Load × perpendicular distance = 100 N x 615 mm

Where θ = tan−1 (y/l)

l = Perpendicular distance from center line to point of load application = 615 mm

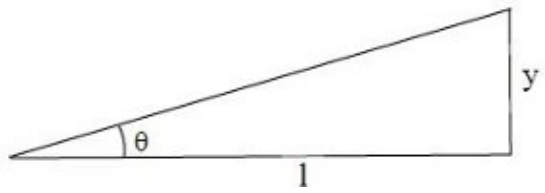


Figure 8. Relationship between applied torque, angular deformation, and deflection.

Figure 8 depicts the methodology used for calculating torsional stiffness, highlighting the geometric relationship between the applied torque, angular deformation, and deflection. The diagram demonstrates how vertical deflection (y) at a point is measured and relates to the perpendicular distance (l) from the chassis centerline to the load application point.

5.0 Physical Testing

To minimize chassis movement during the torsional rigidity test, a specialized fixture system was designed and fabricated[14]. The car was supported on four fixture plates secured to the hubs using three lug bolts, with the plates bolted to C-channels for a stable and rigid testing framework. To eliminate suspension free play, the dampers in the front and rear suspension geometry were replaced with rigid links.

The rigidity of both the front and rear sections of the chassis was evaluated using the following procedure:

1. Rear Chassis Rigidity Testing: The front section of the chassis was fixed to a C-channel using fixture supports bolted to the upright, with a V-block placed beneath the upright for additional stability. At the rear of the chassis, the upright was bolted to a fixture plate, which was then secured to the C-channel.
2. Front Chassis Rigidity Testing: The C-channel at the front was positioned on a V-shaped block placed at the exact center of the channel, allowing it to pivot during the loading process. This configuration ensured that equal force was transmitted in opposite directions on either side of the channel, generating a couple in the rear section of the chassis.
3. To measure deflections, two dial gauges with an accuracy of 0.01 mm were placed beneath the upright. Weights were gradually added to one end, and the corresponding deflections were recorded. This data was used to calculate the overall torsional rigidity of the rear section of the chassis.

Figure 9 shows the physical testing setup used to evaluate chassis torsional rigidity under real- world conditions, featuring a stable fixture system designed to minimize chassis movement and ensure accurate deflection measurements



Figure 9. Physical Testing Setup.

The Torsional stiffness can be obtained based on physical testing by using following equation.

$$k = \frac{T}{\theta} = \frac{F\ x\ l1}{tan^{-1}\left(\frac{\Delta y1 + \Delta y2}{2\ x\ l2}\right)}$$

5.1 Results of Physical Testing

Tables 2 and 3 summarize the deflection data observed during physical testing of the chassis. Table 2 records the displacement measurements for the rear wheels when the front suspension is fixed, while Table 3 captures the deflection data for the front wheels when the rear suspension is fixed. These measurements provide critical input for calculating the torsional stiffness of the chassis.

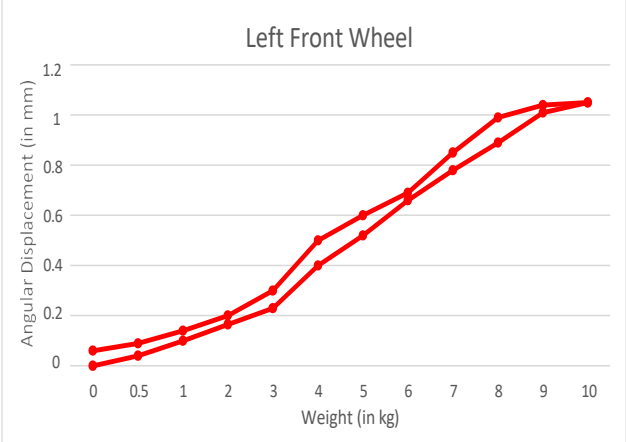


Figure 10. Hysteresis and regression plot for front left wheel.

Table 2. Front fixed Setup displacement

Sr. No.	Weight (kg)	Angular Displacement in y-direction in Left rear wheel (mm)	Angular Displacement in y-direction in Right rear wheel (mm)
1	0	0	0
2	0.5	0.035	0.035
3	1	0.075	0.075
4	2	0.165	0.165
5	3	0.224	0.224
6	4	0.281	0.281
7	5	0.328	0.328
8	6	0.365	0.365
9	7	0.496	0.496
10	8	0.524	0.524
11	9	0.589	0.589
12	10	0.615	0.615

Table 3. Rear fixed setup displacement

Sr. No.	Weight (kg)	Angular Displacement in y-direction in Left front wheel (mm)	Angular Displacement in y-direction in Right front wheel (mm)
1	0	0	0
2	0.5	0.04	0.04
3	1	0.10	0.12
4	2	0.165	0.19
5	3	0.23	0.26
6	4	0.40	0.42
7	5	0.52	0.55
8	6	0.66	0.65
9	7	0.78	0.81
10	8	0.89	0.89
11	9	1.01	1.02
12	10	1.06	1.06

Figures 10 and 11 present the hysteresis and regression plots for the front left and right wheels, respectively. The data for these plots was obtained from Table 3, which records the deflections measured during physical testing. The plots show two lines representing the loading and unloading phases, with the equation $y = 0.073x + 0.127$ derived as an approximation between these two lines. These equations were subsequently used to calculate



Figure 11. Hysteresis and regression plot for front right wheel.

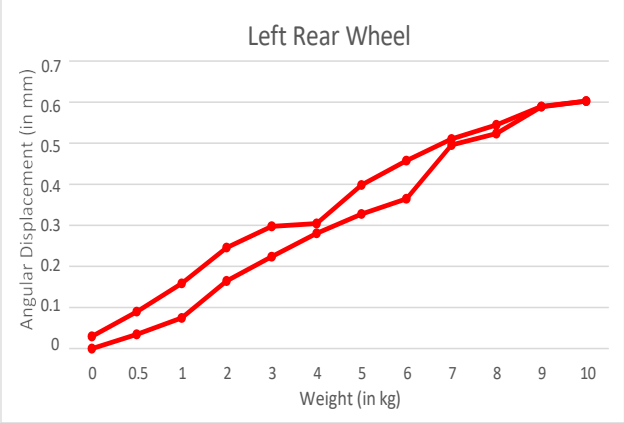


Figure 12. Hysteresis and regression plot for rear left wheel.

the torsional stiffness values for the front section of the chassis, validating the physical testing results. In this equation x and y indicates applied loads and observed displacements respectively.

Figures 12 and 13 illustrate the hysteresis and regression plots for the rear left and right wheels, respectively, based on the deflection data in Table 2. Similar to the front wheels, the plots depict two lines for the loading and unloading phases. The straight-line equation $y = 0.1x + 0.05$ is derived as an approximation between these two lines, providing a linear model for the load- deflection relationship observed during testing of the rear wheels. This approximation helps quantify the

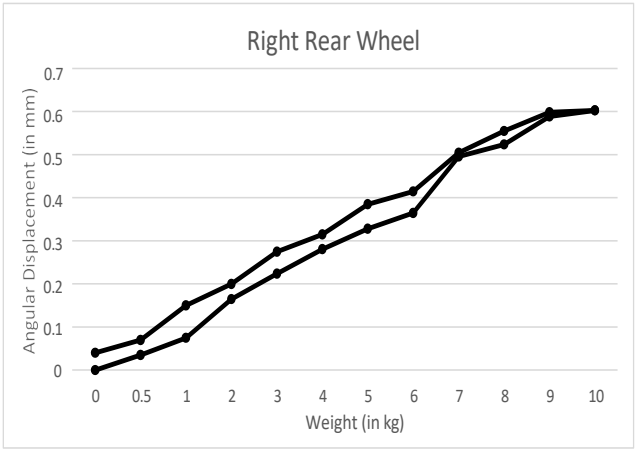


Figure 13. Hysteresis and regression plot for rear right wheel.

torsional response of the chassis. These equations were utilized to compute the torsional stiffness values for the rear section of the chassis, ensuring alignment with the experimental observations[15].

6.0 Observations

The observations from the study indicate a close correlation between the values obtained from FEA (ANSYS APDL) simulations and physical testing. The ANSYS APDL analysis calculated the torsional stiffness of the chassis to be 2580.59 Nm/deg, while the corresponding physical testing yielded a value of 2482.13 Nm/deg (Refer Appendix for the calculation of Torsional stiffness of front and rear suspensions). This minor variance, within an acceptable margin of error, highlights the accuracy and reliability of the simulation approach. The alignment between computational and experimental results validates the use of ANSYS APDL as an effective tool for analyzing and optimizing the torsional rigidity of chassis designs.

Table 4 provides a comparison between the torsional stiffness values obtained through Finite Element Analysis (FEA) in ANSYS APDL and those determined from physical testing. This comparison highlights the strong agreement between computational simulations and experimental methods, validating the reliability and accuracy of the FEA approach for analyzing torsional stiffness in chassis design.

Table 4. Comparison between values of FEA and physical testing

Stiffness Calculation Method	Torsional stiffness of Front suspension (Nm/deg)	Torsional stiffness of Rear suspension (Nm/deg)	Total Torsional Stiffness (Nm/deg)
FEA on ANSYS APDL	950.08	1630.51	2580.59
Physical Testing	911.52	1570.61	2482.13

7.0 Conclusion

This study highlights the effectiveness of FEA using ANSYS APDL in evaluating the torsional rigidity of a Formula Student race car chassis, providing a cost-effective and efficient alternative to traditional physical testing. The analysis allowed for precise modeling of the chassis, incorporating key parameters such as material properties, geometry, and load positioning, enabling the assessment of various design configurations. The use of AISI 1018 steel as the chassis material proved optimal, offering a balance between strength and weight.

The results from FEA were validated through physical testing, with both methods showing strong agreement. This alignment confirms the reliability of the computational model in capturing the torsional behavior of the chassis. The FEA and experimental torsional stiffness values of 2580.59 Nm/deg. and 2482.13 Nm/deg. respectively, underscore the robustness of the design and its suitability for high-performance applications. The minimal variance, within an acceptable margin of error, reinforces the confidence in using simulation tools for chassis optimization.

However, certain limitations must be acknowledged. The simulations assumed idealized boundary conditions and static loading, which may not fully replicate real-world dynamic forces, vibrations, and thermal effects encountered during vehicle operation. The study further assumes material uniformity for AISI 1018 steel, ignoring potential manufacturing variations. Additionally, physical testing is subject to minor inaccuracies due to fixture flexibility and measurement resolution limits. The focus on static torsional rigidity excludes the analysis of fatigue behavior and long-term dynamic effects, which are critical for real racing conditions.

Despite these limitations, the study successfully demonstrates that simulation-based analysis, when combined with experimental validation, offers a robust approach for improving the torsional rigidity of race car chassis. Future research incorporating dynamic analysis, fatigue testing, and the evaluation of weight-to-stiffness trade-offs can further enhance the design process. Overall, the findings underscore the importance of torsional rigidity in achieving optimal handling, stability, and performance in Formula Student vehicles, while providing a strong foundation for further design refinements.

7.1 Future Recommendations

Though the torsional stiffness of a Formula Student chassis made of AISI 1018 steel is effectively assessed and optimized in this study, future research can investigate the use of lightweight materials like aluminum alloys or hybrid composite-metal structures to achieve an improved strength-to-weight ratio[16]. By using sophisticated FEA to investigate topology optimization techniques, the chassis' structural efficiency could be further improved while needless weight is reduced.

Additionally, dynamic vehicle testing should be carried out to validate the effect of chassis stiffness on handling and ride comfort by comparing computational results with actual performance. Since joint compliance can greatly affect overall chassis rigidity, future research may also concentrate on parametric studies of joint stiffness and welding techniques[17]. Incorporating active chassis control systems and assessing how they affect stiffness and load distribution may provide important information for designing vehicles of the future.

Finally, weight reductions and increased customization potential may result from the development of alternative manufacturing techniques like Additive Manufacturing

(AM) for structural components. Future designs can further maximize performance while preserving cost- effectiveness and adherence to Formula Student regulations by implementing these developments.

8.0 References

1. Formula Student Rules; 2025.
2. Rao PK, Putsala KS, Muthupandi M, Mojeswararao D. Numerical analysis on space frame chassis of a formula student race car. Materials Today: Proceedings. 2022; 66:754-9. https://doi.org/10.1016/j.matpr.2022.04.077
3. Reddy NY, Kumar VS. Study of different parameters on the chassis space frame for the sports car by using FEA, IQSR J Mech Civ Eng. 2013; 9(1):1-2. https://doi.org/10.9790/1684-0910109
4. Kumar MP, Muralidharan V. Design and analysis of a tubular space frame chassis of a high performance race car. Int J Res Eng Technol. 2014; 3(02).
5. Guo H, Zhou X, Liu Z. Advanced lightweight structural materials for automobiles: properties, manipulation, and perspective. Sci Adv Mater. 2024; 16(5):563-80. https://doi.org/10.1166/sam.2024.4686
6. Tam NT, Le TP, Huynh NT, Nguyen QM. Optimization of frame structure coach 29/34 seats in static durability state. Eng Sci Technol. 2023; 47:101523. https://doi.org/10.1016/j.jestch.2023.101523
7. Prajwal P, Muralidharan V, Madhusudhana G. Design and analysis of a tubular space frame chassis of a high performance race car. Int J Res Eng Technol. 2014. https://doi.org/10.15623/ijret.2014.0302086
8. Goyal P., and Mehta S. (2021). Impact of structural reinforcements on chassis rigidity. SAE technical paper 2021-01-0987.
9. Riley W, George A. 2002-01-3300 Design, analysis and testing of a formula SAE car chassis. Motorsports Engineering Conference and Exhibition; 2002.https://doi.org/10.4271/2002-01-3300
10. Farabi J. The design and analysis of multiple monocoque chassis for Formula Student (FS) racecar; 2021. p. 19-32.
11. Jain A. Computational analysis and optimization of torsional stiffness of a formula- SAE chassis. SAE Technical Paper 2014-01-0355; 2014.https://doi.org/10.4271/2014-01-0355
12. Rodrigues A, Gertz L, Cervieri A, Poncio ALR, Oliveira A, Pereira M. Static and dynamic analysis of a chassis of a prototype Car. 24th SAE Brasil International Congress and Display; 2015.https://doi.org/10.4271/2015-36-0353
13. Lee C, Park J. Numerical investigation of torsional stiffness in motorsport chassis design. Comput Mech. 2020; 62(3):298-312.
14. Eakambaram A, Baskara S, Saibalaji MA, Baskar A. Experimental analysis and validation of torsional stiffness of a tubular space frame chassis. Mater Today Proc. 2021; 46(17):7719-7727. https://doi.org/10.1016/j.matpr.2021.02.238.
15. Singh H, Verma A. Torsional rigidity testing of automotive frames: A comparison between simulation and experimentation. Engineering Reports. 2022; 35(4):501-519.
16. Brown T, Wilson R. Optimizing space frame chassis design for lightweight performance. Mater Sci Eng. 2021; 55(6):789-803.
17. Fernandez M, Gonzalez J. Influence of tube dimensions on chassis stiffness and safety. Int J Automot Eng. 2021; 49(7):899-912.

Abbreviations

k_{veh}	=	**Total Vehicle Stiffness**
k_{rel}	=	**Relative Stiffness**
k_{ch}	=	**Chassis Stiffness**
k_{susp}	=	**Suspension Stiffness**
k_f & k_r	=	**Stiffnesses of the Front and Rear Suspensions respectively**
k	=	**Torsional Stiffness (Nm/deg)**

T	=	**Torque applied**
y	=	**Vertical Deflection at the Load Application Node**
l	=	**Perpendicular distance from center line to point of load application**
θ	=	**Angular Displacement in y direction**
$y1$ *and* $y2$	=	**Translational Displacement**
$l1$	=	**Distance of Hubs from center of Chassis**
$l2$	=	**Distance of application of load from center of Chassis**

A. Appendix

The Torsional stiffness of front and rear suspension tabulated in the Table 4 is obtained as below.

A.1 Calculation for Torsional Stiffness of the Rear and Front Suspensions

T= Applied Load × perpendicular distance= 100 N x 615 mm
l = 615 mm
l1= 615mm
l2= 900mm

A.1.1 Rear Stiffness Calculations

a). Using Angular Displacement from Finite Element Analysis (ANSYS APDL)
y = 0.40486 mm
θ= tan-1 (y/l) = tan-1(0.40486/615) = 0.03771 deg

$$k = \frac{T}{\theta} = \frac{100 * 615 * 10^{-3}}{0.03771} = 1630.51 \text{ N m/d eg}$$

b). Using Angular Displacement from Result of Physical Testing

$$k = \frac{T}{\theta} = \frac{F\ x\ l1}{tan^{-1}\left(\frac{\Delta y1 + \Delta y2}{2\ x\ l2}\right)}$$

y1 and y2 = 0.615 mm

$$k = \frac{F\ x\ l1}{tan^{-1}\left(\frac{\Delta y1 + \Delta y2}{2\ x\ l2}\right)} = \frac{100 * 615 * 10^{-3}}{tan^{-1}\left(\frac{0.615 + 0.615}{2\ x\ 900}\right)}$$

$$= 1570.61\ N\,m/d\,eg$$

A.1.2 Front Stiffness Calculations

a). Using Angular Displacement from Finite Element Analysis (ANSYS APDL)
y = 0.6948 mm
θ= tan-1 (y/l) = tan-1(0.6948/615) = 0.06473 deg

$$k = \frac{T}{\theta} = \frac{100 * 615 * 10^{-3}}{0.06473} = 950.08 \text{ N m/d eg}$$

b). Using Angular Displacement from Result of Physical Testing

$$k = \frac{T}{\theta} = \frac{F\ x\ l1}{tan^{-1}\left(\frac{\Delta y1 + \Delta y2}{2\ x\ l2}\right)}$$

$$k = \frac{F\ x\ l1}{tan^{-1}\left(\frac{\Delta y1 + \Delta y2}{2\ x\ l2}\right)} = \frac{100 * 615 * 10^{-3}}{tan^{-1}\left(\frac{1.06 + 1.06}{2 * 900}\right)}$$

$$= 911.52\ N\,m/d\,eg$$